Bakker A., Fasano J.B. (1993) *Time Dependent, Turbulent Mixing and Chemical Reaction in Stirred Tanks.* Annual AIChE Meeting, November 1993, St. Louis, Missouri. AIChE Symposium Series 299, Volume 90, 1993, page 71-78.

Time Dependent, Turbulent Mixing and Chemical Reaction in Stirred Tanks

André Bakker and Julian B. Fasano
Chemineer, Inc., 5870 Poe Ave., Dayton, OH 45401

Blend time and chemical product distribution in turbulent agitated vessels can be predicted with the aid of Computational Fluid Mixing (CFM) models. The blend time predictions show good agreement with an experimental correlation. Calculations for turbulent, time dependent mixing of two chemicals, exhibiting a competitive pair of reactions, are compared with experimental results. The effects of the position of the inlet feed stream in the turbulent flow field are studied. It is concluded that process problems with turbulent chemical reactors can be avoided by incorporating the results of CFM simulations in the design stage.

INTRODUCTION

Blending of chemical reactants is a common operation in the chemical process industries. Blend time predictions are usually based on empirical correlations. When a competitive side reaction is present, the final product distribution is often unknown until the reactor is built. The effects of the position of the feed stream on the reaction byproducts are usually unknown. Also, the scale up of chemical reactors is not straightforward. Thus, there is a need for comprehensive, physical models that can be used to predict important information like blend time and reaction product distribution, especially as they relate to scale and feed position.

The objective of this paper is to investigate the extent to which Computational Fluid Mixing (CFM) models can be used as a tool in the design of industrial reactors. The commercially available program Fluent™ is used to calculate the flow pattern and the transport and reaction of chemical species in stirred tanks. The blend time predictions are compared with a literature correlation for blend time. The product distribution for a pair of competing chemical reactions is compared with experimental data from the literature.

MODEL

The flow pattern is calculated from conservation equations for mass and momentum, in combination with the Algebraic Stress Model (ASM) for the turbulent Reynolds stresses, using the Fluent V3.03 solver. These equations can be found in numerous textbooks and will not be reiterated here. Once the flow pattern is known the mixing and transport of chemical species can be calculated from the following model equation:

$$\frac{\partial}{\partial t}(\rho X_i) + \frac{\partial}{\partial x_j}(\rho u_j X_i) = \frac{\partial}{\partial x_j}\left(\frac{\mu_t}{Sc_t}\frac{\partial X_i}{\partial x_j}\right) + R_i \qquad (1)$$

Here X_i is the mass fraction of chemical species i and R_i is the rate of creation or depletion by chemical reaction. For a single step, first order reaction like A + B → R the reaction rate is given by:

$$R_i \propto \left(C_A C_B + \overline{c_A c_B}\right) \qquad (2)$$

Here C_A and C_B (upper case) denote the mean molar concentrations of reactants A and B while c_A and c_B (lower case) denote the local concentration fluctuations that result from turbulence. When the species are perfectly mixed the second term on the right hand side, containing the correlation of the concentration fluctuations, will approach zero. Otherwise, if the species are not perfectly mixed, this term will be

negative and will reduce the reaction rate. The estimation of this correlation term is not straightforward and numerous models are available. An excellent discussion on this subject was given by Hannon [1].

The model used here is a slightly modified version of the standard Fluent model [2]. Two possible reaction rates are calculated, the kinetic reaction rate R_{ki} and a second reaction rate R_{mi} that is controlled by the turbulent mixing. The kinetic reaction rate for species i is calculated as:

$$R_{ki} = KM_i \prod_{j\ reactants} \frac{\rho X_j}{M_j} \qquad (3)$$

The turbulent mixing limited reaction rate for species i is calculated as:

$$R_{mi} = \left(M_i A_{mn} \frac{\epsilon}{k}\right) \cdot minimum\left(\left(\frac{\rho X_j}{v_j M_j}\right)_{reactants\ j}\right) \qquad (4)$$

The "minimum" function gives the minimum value of $(\rho.X_j/v_j.M_j)$ of all the reactants j taking part in this reaction. Finally the reaction rate R_i is calculated as the product of the molar stoichiometry v_i of species i and the minimum of R_{ki} and R_{mi}:

$$R_i = -v_i\ minimum(R_{mi}, R_{ki}) \qquad (5)$$

Here M_i is the molecular weight of species i and A_{mn} is an empirically determined model constant for reaction n. In the reaction system studied here, v_i is +1 for reactants and -1 for products. K is the kinetic rate constant of the reaction.

The idea behind this model is that in regions with high turbulence levels the eddy lifetime k/ϵ will be short, mixing fast and as a result the reaction rate is not limited by small scale mixing. On the other hand, in regions with low turbulence levels, small scale mixing may be slow and limit the reaction rate.

RESULTS REACTION MODELING

The following competitive-consecutive reaction system was studied:

$$A + B \xrightarrow{K_1} R$$

$$B + R \xrightarrow{K_2} S$$

This is the reaction system used by Bourne *et al.* [3] and Middleton *et al.* [4]. The first reaction is much faster than the second reaction: K_1 = 7300 $m^3.mole^{-1}.s^{-1}$ vs. K_2 = 3.5 $m^3.mole^{-1}.s^{-1}$. The experimental data published by Middleton *et al.* were used to determine the model constant A_{mn}. Two reactors were studied, a 30 l reactor equipped with a D/T=1/2 D-6 impeller and a 600 l reactor with a D/T=1/3 D-6 impeller. A small volume of reactant B was instantaneously added just below the liquid surface in a tank otherwise containing reactant A. A and B were added on an equimolar basis. The transport, mixing and reaction of the chemical species were then calculated using the flow pattern in Figure 1 as a basis. Experimental data were used as impeller boundary conditions. The product distribution X_s is then calculated as:

$$X_s = \frac{2C_S}{C_R + 2C_S} \qquad (6)$$

In the reaction model used here it was assumed that small scale mixing only affected the first reaction and that once this reaction had occurred, the species were locally well mixed. As a result, small scale turbulent mixing did not affect the second reaction. This was achieved by using different values of A_{mn} for both reactions. For the second reaction A_{m2} was set to infinity. The value for A_{m1} was then varied, to study the effect on the predicted final product distribution.

Figure 2 shows the predicted X_s as a function of A_{m1} for the 30 l reactor at 100 RPM. Decreasing A_{m1} slows down the first reaction and increases the formation of the secondary product S. As a result the predicted X_s decreases with increasing A_{m1}. It was found that A_{m2} = 0.08 gave the best predictions, when compared to the experimental data from Middleton *et al.* Figure 3 shows a comparison between the experimental data from Middleton *et al.* and the current model predictions for both the 30 l and the 600 l reactors. X_s is plotted as a function of RPM. This graph shows that the model predicts the effects of scale and impeller rotational speed correctly, and is usually within 10% of the experimental results.

The effect of inlet position of the feed stream on the formation of the secondary by-product S was studied. Figure 4 shows values of X_s for various feed locations. X_s varies only slightly when the inlet is located in the fluid bulk. However, when the feed is injected directly above the impeller, such that the feed stream immediately passes through the highly turbulent impeller zone, local mixing is much faster and does not limit the rate of the first reaction. As a result there is less reaction by-product S and the final X_s is only 50% of what it would be if the feed were located away from the impeller. This qualitatively agrees with the experimental results of Tipnis *et al.* [5]. Tipnis *et al.* used a different set of reactions and different tank geometries but also found that injection near the impeller results in a lower X_s than injection farther away from the impeller and that the relative differences are similar to those found in this study.

Figure 5 shows the concentrations of R and S and the product distribution X_s as a function of time for the feed location just above the impeller. The values are normalized with respect to the final values. R and S increase steadily with time. X_s increases at first, reaching a local maximum just before the species are mixed by the impeller. The improved quality of the mixture favors the first reaction and X_s drops, until it reaches a local minimum. At this point there is enough R present to allow the second reaction to occur even in relatively well mixed regions, and X_s increases again until it asymptotically reaches a final value. Figures 6a-h show the local concentrations of species A, R and S as a function of time for the 600 l tank at 100 RPM.

BLEND TIME

The mixing of two non-reacting species in a tank equipped with a high efficiency impeller (Chemineer HE-3) impeller was calculated using Fluent V3.03. The tank diameter was T = 1 m. Further Z/T = 1; D/T = 0.33; C/T = 0.32 and RPM = 58. The flow pattern in this tank is shown in Figure 7. Experimental data were used as impeller boundary conditions. Figure 8 shows the uniformity of the tank as a function of time. The model predictions are compared with the results of the experimental blend time correlation of Fasano and Penney [6]. This graph shows that for a uniformity above 90% there is excellent agreement between the model predictions and the experimental correlation. Figure 9a shows the concentration field at t = 0 s. Figures 9b-d show the concentration field at t = 4 s, t = 10 s and t = 20 s respectively. After 80 s the species are homogeneously mixed.

DISCUSSION

The models presented here correctly predicts blend time and reaction product distribution. The reaction model correctly predicts the effects of scale, impeller speed and feed location. This shows that such models can provide valuable tools for designing chemical reactors. Process problems may be avoided by using CFM early in the design stage. When designing an industrial chemical reactor it is recommended to determine the values of the model constants on a laboratory scale. The reaction model can then be used to optimize the product conversion on the production scale varying agitator speed and feed position.

However, the range of validation of the reaction model was limited. Only one impeller type and one reaction system were studied. Future work has to concentrate on testing the model for a wider range of geometries and reaction systems, and if necessary modify the model to increase it's range of validity.

LITERATURE

[1] Hannon, J., 1992, *Mixing and Chemical Reaction in Tubular Reactors and Stirred Tanks*, Ph.D. Thesis, Cranfield Institute of Technology, U.K.

[2] Fluent V3.03 Users Manual, 1990, Fluent Inc., Lebanon NH

[3] Bourne, J.R., Kozicki, F., Rys, P., 1981, *Mixing and Fast Chemical Reaction - I; Test Reactions to Determine Segregation*, Chem. Eng. Sci., 36(10)1643

[4] Middleton, J.C., Pierce, F., Lynch, P.M., 1986, *Computations of Flow Fields and Complex Reaction Yield in Turbulent Stirred Reactors and Comparison with Experimental Data*, Chem. Eng. Res. Des., Vol 64, January 1986, pp. 18-21

[5] Tipnis, S.K., Penney, W.R. Fasano, J.B., 1993, *An Experimental Investigation to Determine a Scale-Up Method for Fast Competitive Parallel Reactions in Agitated Vessels*, AIChE Annual Meeting, November 1993, St. Louis

[6] Fasano, J.B., Penney, W.R., 1991, *Avoid Blending Mix-Ups*, Chemical Engineering Progress, October 1991, 56-63

SYMBOLS

A_{mn}	Model constant for reaction n
C_i	Concentration of species i (mole m^{-3})
k	Turbulent kinetic energy density (m^2 s^{-2})
K	Reaction rate constant (m^3 $mole^{-1}$ s^{-1})
M_i	Molecular weight species i
R_i	Production/depletion species i (kg m^{-3} s^{-1})
R_{ki}	Kinetic reaction rate species i (kg m^{-3} s^{-1})
R_{mi}	Mixing limited reaction rate for species i (kg m^{-3} s^{-1})
Sc_t	Turbulent Schmidt number
t	Time (s)
u_i	Velocity in direction i (m s^{-1})
x_i	Spatial coordinate in direction i (m)
X_s	Product distribution
X_i	Mass fraction species i
ϵ	Turbulent kinetic energy dissipation rate density (m^2 s^{-3})
μ_t	Turbulent viscosity (kg m^{-1} s^{-1})
ρ	Liquid density (kg m^{-3})
ν_i	Stoichiometry species i

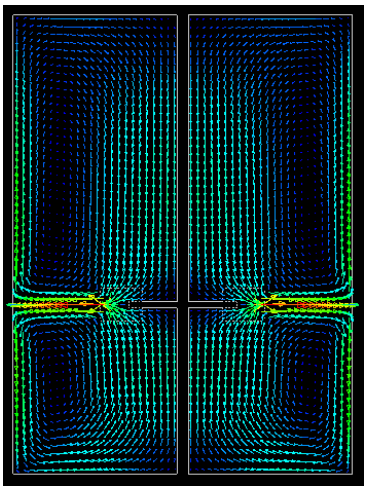

Figure 1 – Flow field in 30 liter reactor.

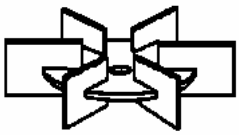

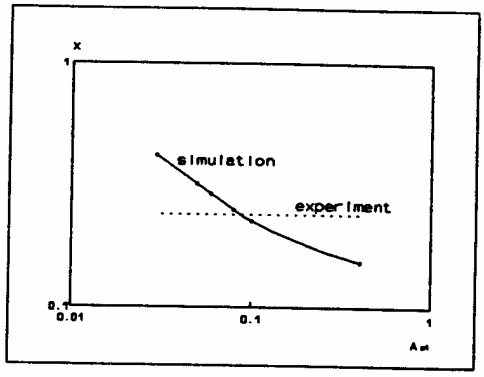

Figure 2 - Predicted X_s vs. A_{m1} for $A_{m2} = \infty$ 30 Liter Reactor at 100 RPM

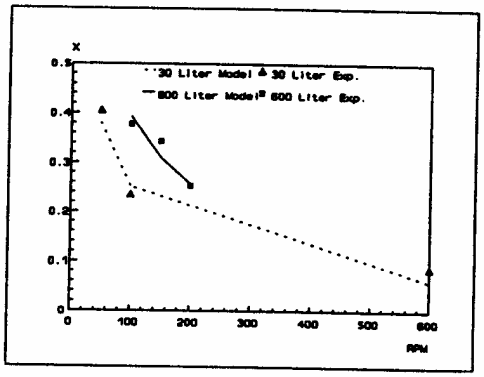

Figure 3 - X_s as a function of RPM. Model predictions compared with data from Middleton *et al.* [4].

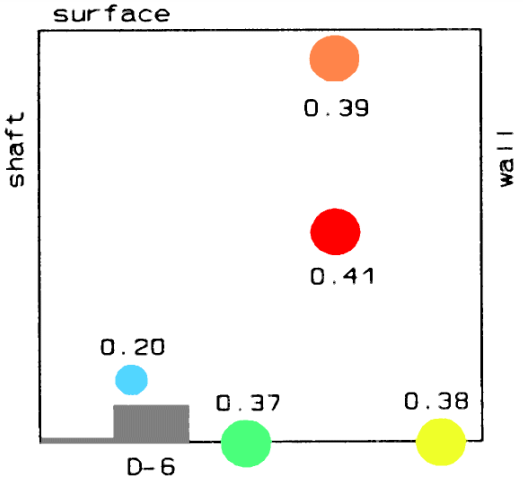

Figure 4 – X_s as a function of feed location. 600 Liter vessel at 100 RPM. A_{m1}=0.08 and $A_{m2} = \infty$.

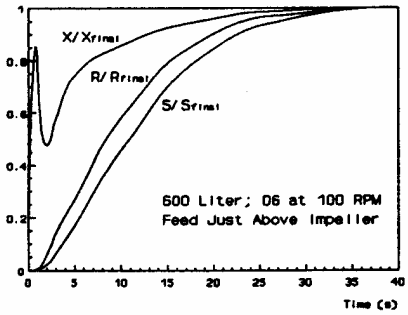

Figure 5 - Concentrations of R and S and product distribution X_s as a function of time, normalized with final values.

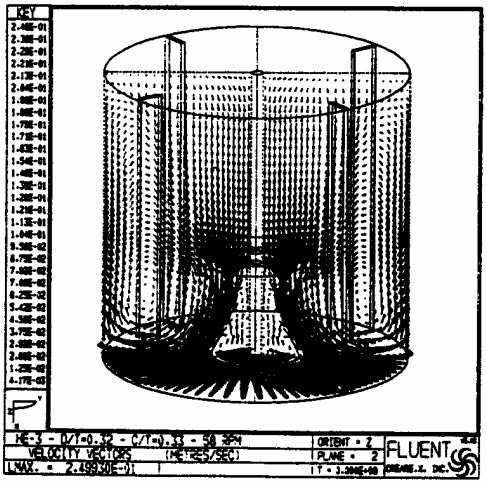

Figure 7 - Flow pattern in tank with a high efficiency impeller (Chemineer HE-3).

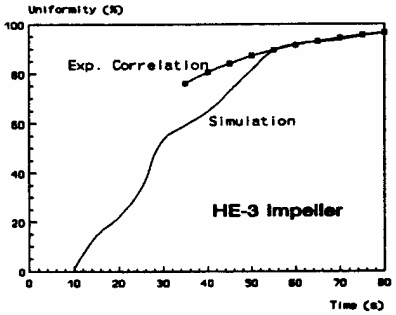

Figure 8 - Uniformity as a function of time.

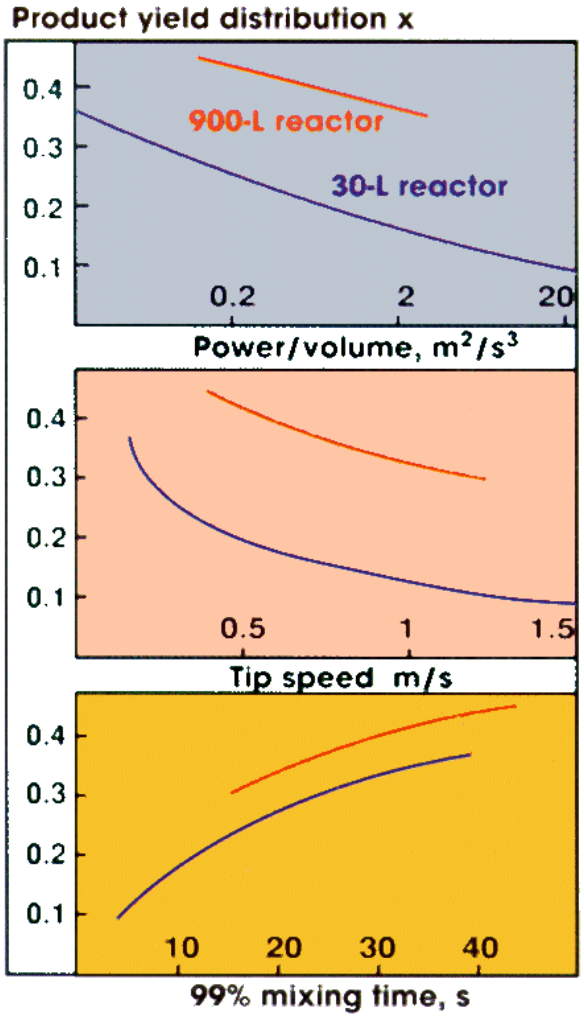

- The efficiency of the reactor can be measured by the product distribution X:

$$X = \frac{2(S)}{(R) + 2(S)}$$

- Three different scale-up criteria were tested by Middleton et al. (Chem. Eng. Res. Des. Vol. 64, January 1986, pp. 18-22):
  - constant power input per volume,
  - constant impeller tip speed,
  - constant mixing time.
- None of these three commonly used criteria was successful in scaling up the reactor to give the same product distribution.

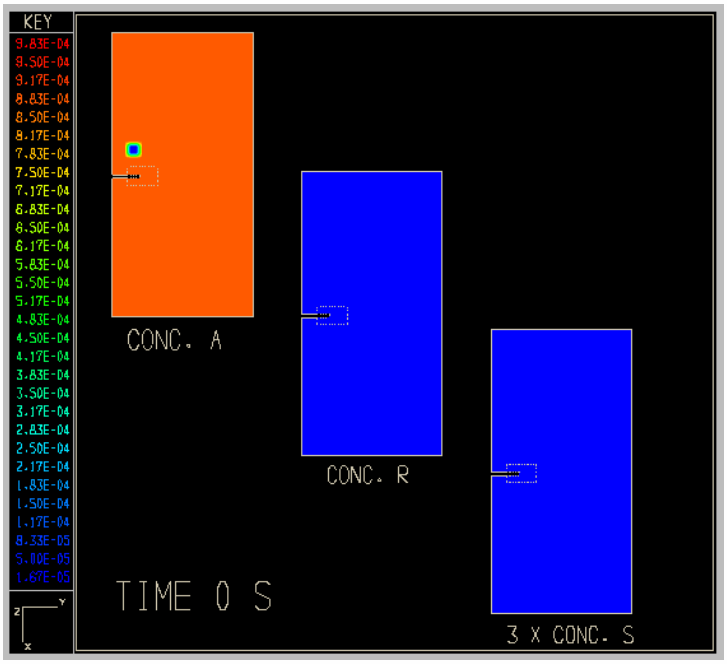

Figure 6a Concentration Field at Time = 0 s

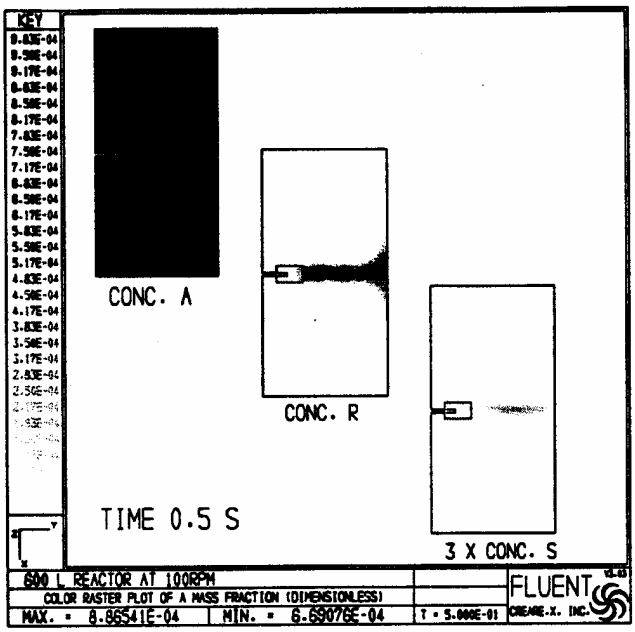

Figure 6b Concentration Field at Time = 0.5 s

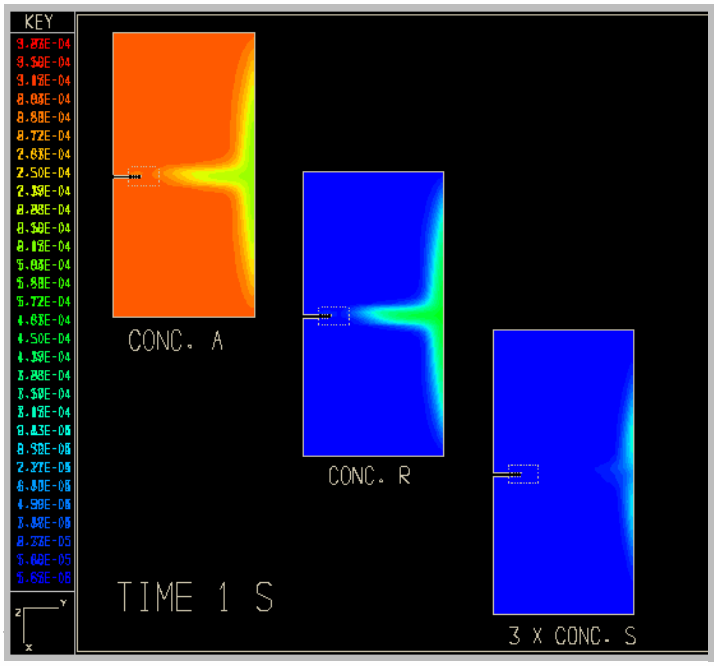

Figure 6c Concentration Field at Time = 1 s

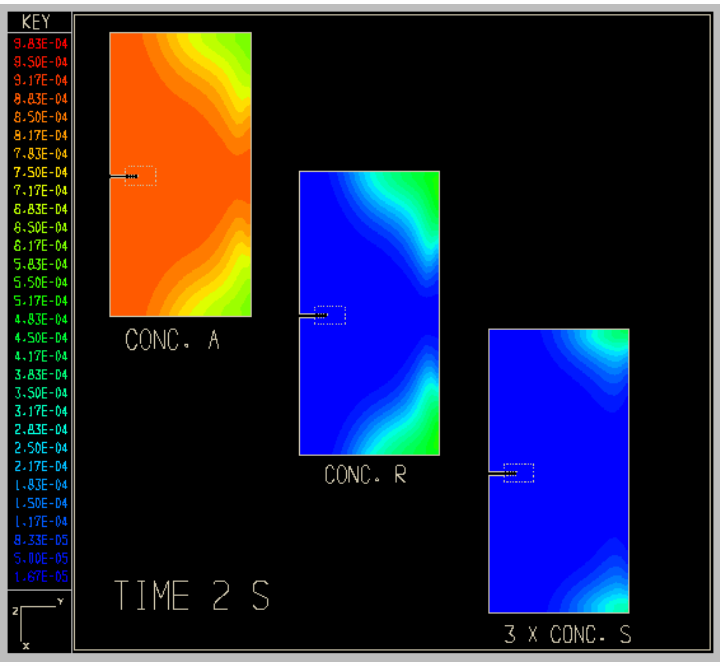

Figure 6d Concentration Field at Time = 2 s

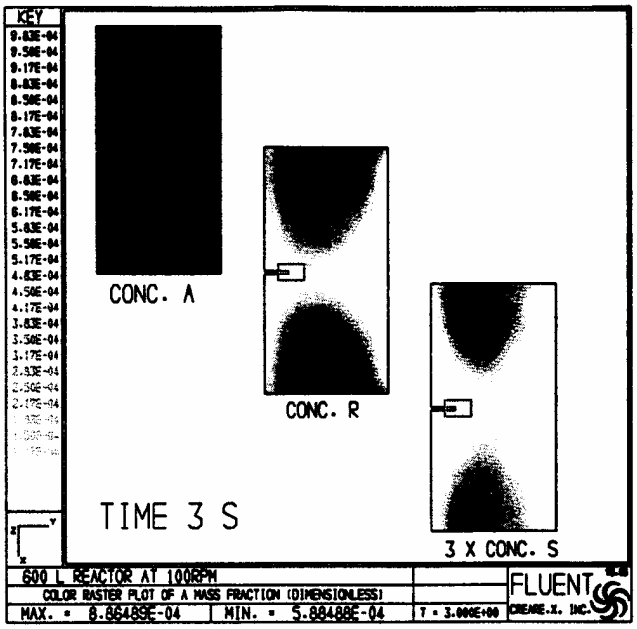

Figure 6e Concentration Field at Time 3 s

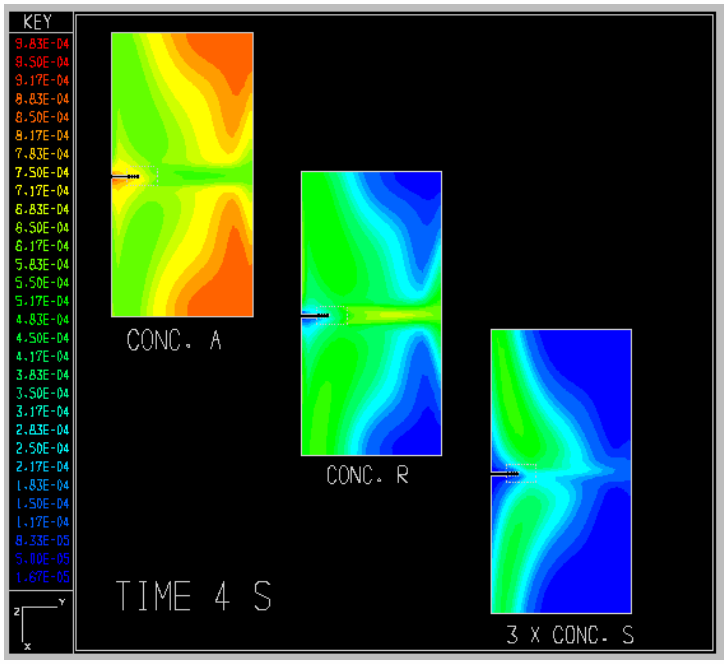

Figure 6f Concentration Field at Time 4 s

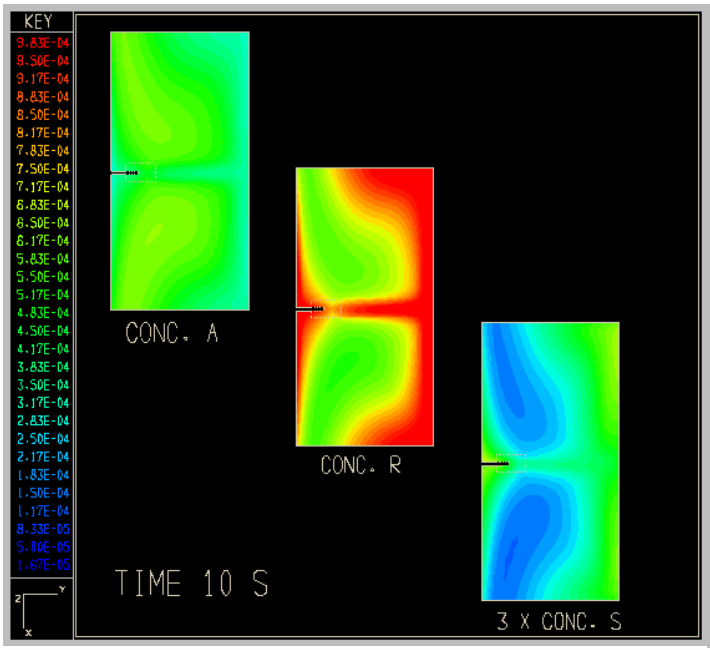

Figure 6g Concentration Field at Time 10 s

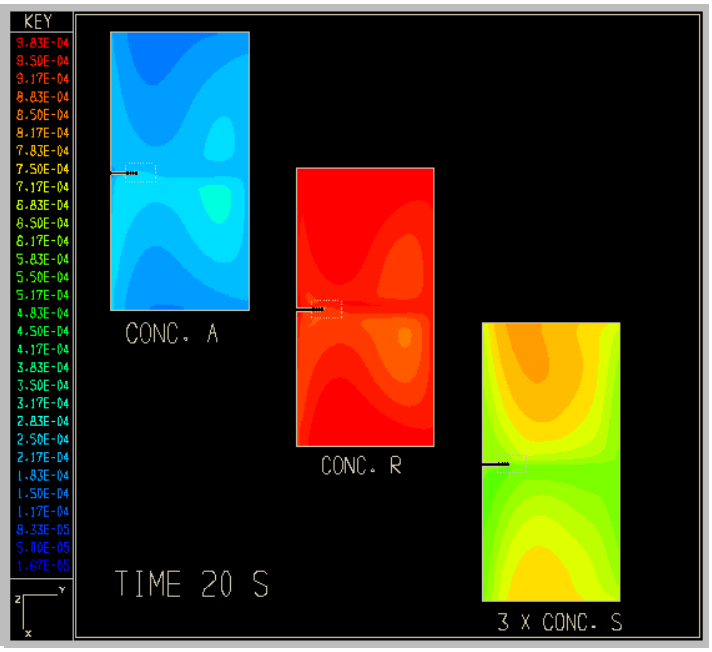

Figure 6h Concentration Field at Time 20 s

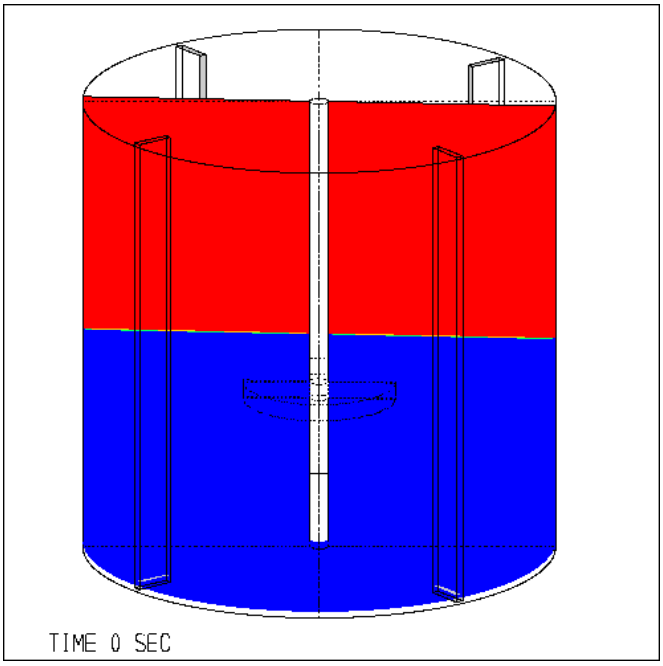

Figure 9a Concentration Field at Time 0 s

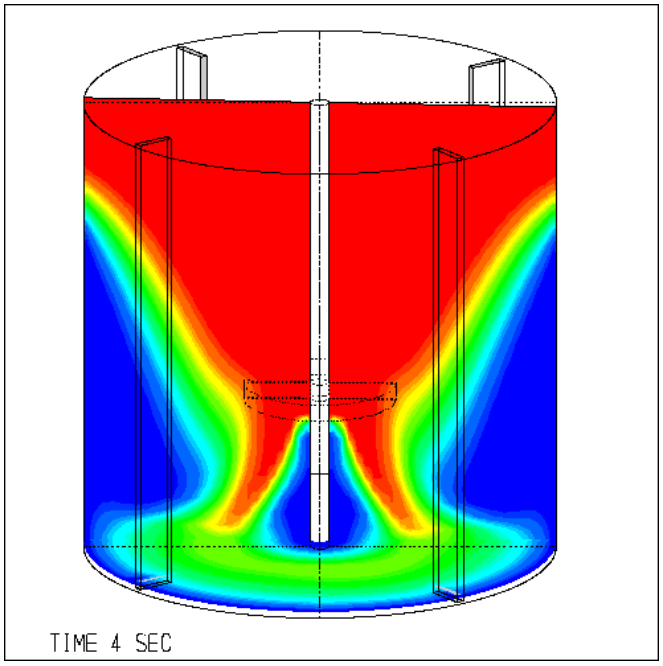

Figure 9b Concentration Field at Time 4 s

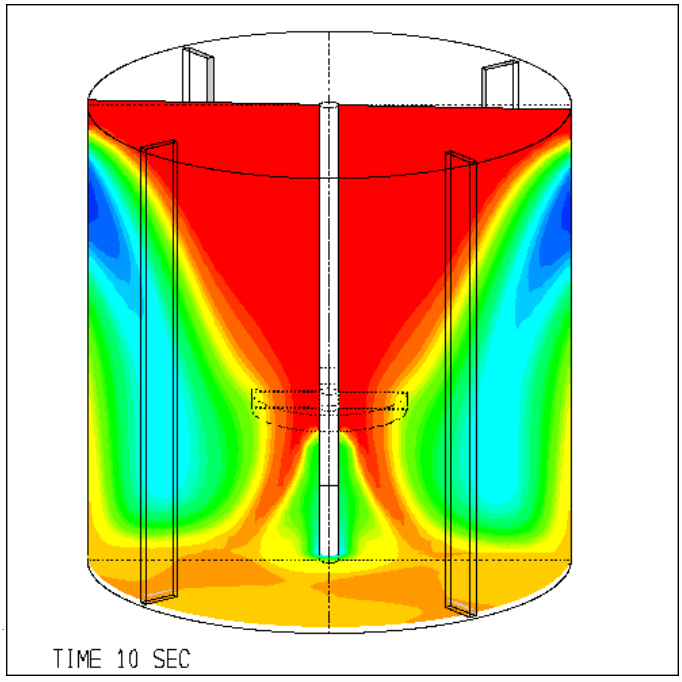

Figure 9c Concentration Field at Time 10 s

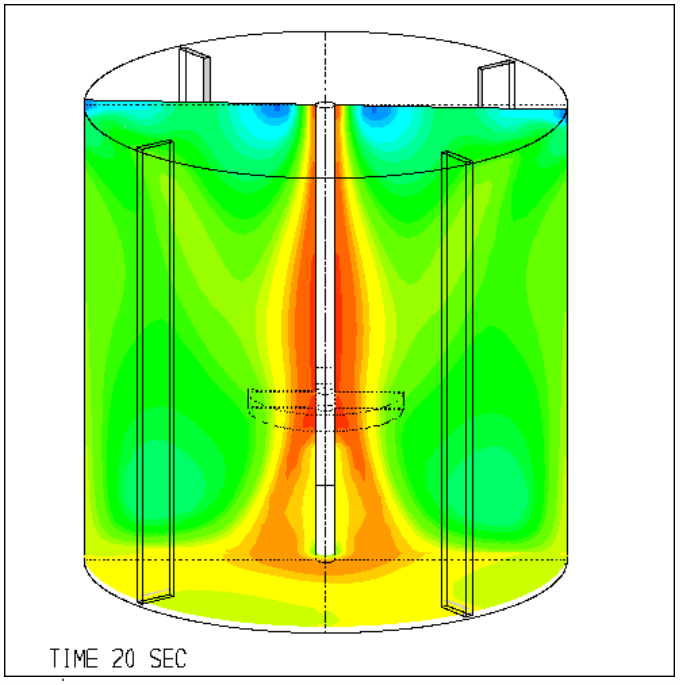

Figure 9d Concentration Field at Time 20 s